

---

## Original Articles

---

# Myocardial Postischemic Injury Is Reduced by PolyADPribose Polymerase-1 Gene Disruption

Andrew A. Pieper<sup>1\*</sup>, Thorsten Walles<sup>2\*</sup>, Guo Wei<sup>2</sup>, Emily E. Clements<sup>3</sup>,  
Ajay Verma<sup>3</sup>, Solomon H. Snyder<sup>1</sup>, and Jay L. Zweier<sup>2</sup>

<sup>1</sup>Departments of Neuroscience, Pharmacology & Molecular Science, and Psychiatry, The Johns Hopkins University School of Medicine, Baltimore, Maryland, U.S.A.

<sup>2</sup>Molecular and Cellular Biophysics Laboratories, Department of Medicine, Division of Cardiology and the Electron Paramagnetic Resonance Center, The Johns Hopkins University School of Medicine, Johns Hopkins Bayview Medical Center, Baltimore, Maryland, U.S.A.

<sup>3</sup>Uniformed Services University of the Health Sciences, Bethesda, Maryland, U.S.A.

Communicated by S. Snyder. Accepted December 21, 1999.

---

### Abstract

**Background:** PolyADPribose polymerase (PARP) is activated by DNA strand breaks to catalyze the addition of ADPribose groups to nuclear proteins, especially PARP-1. Excessive polyADPriboseylation leads to cell death through depletion of NAD<sup>+</sup> and ATP.

**Materials and Methods:** In vivo PARP activation in heart tissue slices was assayed through conversion of [<sup>3</sup>P]NAD<sup>+</sup> into polyADPribose (PAR) following ischemia-reperfusion (I/R) and also monitored by immunohistochemical staining for PAR. Cardiac contractility, nitric oxide (NO), reactive oxygen species (ROS), NAD<sup>+</sup> and ATP levels were examined in wild type (WT) and in PARP-1 gene-deleted (PARP-1<sup>-/-</sup>) isolated, perfused mouse hearts. Myocardial infarct

size was assessed following coronary artery occlusion in rats treated with PARP inhibitors.

**Results:** Ischemia-reperfusion (I/R) augmented formation of nitric oxide, oxygen free radicals and PARP activity. I/R induced decreases in cardiac contractility and NAD<sup>+</sup> levels were attenuated in PARP-1<sup>-/-</sup> mouse hearts. PARP inhibitors reduced myocardial infarct size in rats. Residual polyADPriboseylation in PARP-1<sup>-/-</sup> hearts may reflect alternative forms of PARP.

**Conclusions:** PolyADPriboseylation from PARP-1 and other sources of enzymatic PAR synthesis is associated with cardiac damage following myocardial ischemia. PARP inhibitors may have therapeutic utility in myocardial disease.

\*Contributed equally to this work.

Address correspondence and reprint requests to: Dr. Jay L. Zweier, Johns Hopkins Asthma and Allergy Center, 5501 Hopkins Bayview Circle, LA.14, Baltimore, MD 21224, U.S.A. Phone: 410-550-0339; Fax: 410-550-2448; E-mail: jzweier@jhmi.edu or Dr. S. H. Snyder, Johns Hopkins University, School of Medicine, 725 N. Wolfe St., Baltimore, MD 21205, U.S.A. Phone: 410-955-3024; Fax: 410-955-3623; E-mail: ssnyder@jhmi.edu

---

### Introduction

Nuclear polyADPribose polymerase (PARP) is activated by DNA strand breaks to transfer up to 200 ADPribose groups from NAD<sup>+</sup> to nuclear proteins, most notably PARP-1. Although polyADPriboseylation is important in base excision repair (1–5), massive DNA damage rapidly leads to PARP-mediated NAD<sup>+</sup> depletion (6). The cell dies from energy loss as ATP is consumed in efforts to resynthesize NAD<sup>+</sup> (7). PARP inhibitors protect against cell death, as does targeted deletion of the PARP-1 gene

(7). For example, streptozotocin killing of pancreatic islet cells, a model of type I diabetes, is abolished in PARP-1 gene-deleted (PARP-1<sup>-/-</sup>) mice (8–10). Furthermore, cerebral ischemic damage is reduced dramatically in PARP-1<sup>-/-</sup> mice (11,12) and in animals treated with PARP inhibitors (13,14). PARP inhibitors reduce in vitro damage to cardiomyoblasts elicited by H<sub>2</sub>O<sub>2</sub>, peroxyntirite and nitric oxide (NO) (15–17), as well as in vivo cardiac reperfusion injury (17–20). PARP inhibition also reduces contractile dysfunction and preserves energy levels following Ischemia-reperfusion (I/R) of isolated perfused rat hearts (21). PARP-1<sup>-/-</sup> hearts are similarly protected (22,23).

In this study, we directly demonstrate in vivo activation of PARP following myocardial I/R associated with increased oxygen radical and nitric oxide generation. Substantial PARP activity following I/R in PARP-1<sup>-/-</sup> mouse heart appears to reflect activation of alternative isoforms of PARP. Cardiac damage is reduced substantially by PARP inhibitors and in PARP-1<sup>-/-</sup> hearts, establishing a relationship between PARP activation, NAD<sup>+</sup> and ATP depletion, and tissue damage.

## Materials and Methods

### Materials

All chemicals or solvents were purchased from Sigma Chemical Co. (St. Louis, MO) unless noted otherwise. [<sup>33</sup>P] NAD<sup>+</sup> was generously donated by NEN Life Science Products (Boston, MA). *N*-methyl-D-glucamine dithiocarbamate (MGD) was synthesized as described previously (24). *N*-methyl-D-glucamine and carbon disulfide required for MGD synthesis were purchased from Aldrich (Milwaukee, WI) and 5,5-dimethyl-1-pyrroline-*N*-oxide (DMPO) was purchased from OMRF (Oklahoma City, OK). GPI 6150 was provided by Guilford Pharmaceuticals (Baltimore, MD). Pentobarbital and heparin were obtained from Abbott Laboratories (Chicago, IL) and Elkins-Sinn, Inc. (Cherry Hill, NJ) respectively.

### Animals

PARP-1<sup>-/-</sup> mice, obtained from Z.Q. Wang (International Agency for Research in Cancer, Leon, France), were created by the homologous recombination of embryonic stem cells using SV 129 mice (25). Brother-sister mating of heterozygous animals with a disrupted PARP-coding gene delivered PARP-1<sup>-/-</sup> mice, which were identified by Southern blotting of tail DNA. Animal lines

were established from four founders. The control WT animals had the same genetic background (129/SvrC57BL/6) as PARP-1<sup>-/-</sup> mice.

### Isolated Mouse Heart Perfusion

Contractile function, energetic state, radical generation, and cell death were examined in isolated perfused mouse hearts (26). PARP-1<sup>-/-</sup> and WT SV129 mice (12 weeks old) were heparinized and anesthetized with pentobarbital intraperitoneally (i.p.). Hearts were rapidly excised and placed in ice cold, oxygen-bubbled Krebs-bicarbonate buffer (120 mM NaCl, 17 mM glucose, 25 mM NaHCO<sub>3</sub>, 5.9 mM KCl, 1.2 mM MgCl<sub>2</sub>, 2.5 mM CaCl<sub>2</sub>). The ascending aorta was cannulated under stereomicroscopy and perfused at 37°C with a constant pressure of 70 mm Hg. Contractile function was assessed by inserting a fluid-filled balloon into the left ventricle (LV) through the mitral valve and securing this balloon with a ligature around the hydraulic line. The balloon was initially inflated to an end-diastolic pressure of 4–8 mm Hg. All subsequent measurements of LV pressure (LVP) were made at this same end-diastolic volume. Cardiac parameters including heart rate, LVP and coronary flow (measured via a Transonic HT107 flowmeter Ithaca, NY) were continuously recorded and stored on a MacLab system (CB Sciences, Inc., Milford, Ma). After cannulation, hearts were equilibrated for 15 min to reach stable function before recording basal values. For PolyADPribose (PAR) immunohistochemistry, PolyADPribose in situ (PARIS) and in situ end labeling (ISEL) myocardial reperfusion lasted 10 min. SC-55858, a superoxide dismutase analog, was infused over 1 min at the end of the equilibration period before onset of global ischemia and during the 10 min reperfusion period, with a final concentration in the isolated heart of 40 μM. L-NAME was infused continuously at a rate of 5% of coronary flow during the last 5 min of the equilibration period before onset of ischemia, for a final concentration in the isolated heart of 1 mM. After reperfusion, hearts were immediately frozen for subsequent analysis. Triplicate hearts were studied for each condition.

### NMR Spectroscopy

Pulsed Fourier transform [<sup>31</sup>P]NMR spectra were obtained on isolated perfused mouse hearts placed in 10-mM NMR tubes, with all requisite lines secured to an attached support rod. Spectra were recorded on a Bruker MSL

500 (Bruker, Karlsruhe, Germany) at a  $^{31}\text{P}$  resonance frequency of 202.46 MHz using a 10-mM broadband probe with proton decoupling. 10 min spectral acquisitions were performed from 600 summed-free induction decays with 1-sec interpulse delay.

#### *In Vivo Regional Myocardial Ischemia In Rat*

Female Sprague Dawley rats (250–300 g) were anesthetized with pentobarbital (45 mg/kg i.p.) and subjected to tracheotomy, intubation and central venous line placement in the right internal jugular vein as previously described (27). Rats were ventilated using a Harvard apparatus rodent ventilator. The chest was opened in the parasternal line with mechanical ventilation with 30% oxygen / 70% room air mixture. A 5-0 polypropylene thread snare was placed around the proximal left anterior descending coronary artery (LAD) and clamped for 45 min. Perfusion was accomplished by releasing the ligation snare. After 2 hr, hearts were rapidly excised and processed for infarct size measurement. In three additional experiments, we examined myocardial protection from I/R with PARP inhibitors. 3-aminobezamide or 4-aminobenzamide (10 mg/kg, dissolved in physiologic saline) were injected into the right jugular vein 1 min before left coronary ligation and 1 min before reperfusion. GPI 6150 (4 mg/kg in dimethylsulfoxide; DMSO) was injected (i.p.) 2 hr before ischemia. Possible drug-related circulatory side effects were ruled out.

#### *Infarct Size Measurement*

Myocardial infarction in isolated mouse hearts was measured by triphenyltetrazolium chloride (TTC, Sigma Chemical Co.) staining of heart sections (28) after 30 min of ischemia, followed by 120 min of reperfusion. Hearts sections (1.5 mm) were stained with 1% TTC, which stains viable myocardium red and infarcted myocardium white. For in vivo studies of myocardial infarction, rats were subjected to LAD occlusion for 45 min, followed by 2 hr of reflow, with 7 rats/group. Risk region was determined by reocclusion of the LAD with monastral blue dye injection into the left atrium. Computerized planimetry of each section was used to determine percent infarction from the mass-weighted average of the ratio of infarct area to the total cross-sectional area of the ventricle.

#### *Immunohistochemical Staining for PAR*

After 30 min global ischemia (mouse) or 45 min regional ischemia (rat) and 10 min reperfusion, hearts were perfused with ice-cold 4% paraformaldehyde-sodium phosphate buffer solution (pH 7.4). Heart sections (40  $\mu\text{m}$ ) were incubated for 48 hr in polyclonal anti-guinea pig PAR (Trevigen) at 1:50 dilution. Biotin-SP-conjugated goat anti-guinea pig (Vector Laboratories, Burlingame, CA) was used as secondary antibody at 1:100 dilution. For signal amplification, an immunoperoxidase ABC kit (Vector Laboratories) was used. Diaminobenzidine was used as a chromogen (Gibco BRL Grand Island, NY). Triplicate hearts were studied for each condition and representative results are shown (Figs. 2 and 4).

#### *Electron Paramagnetic Resonance (EPR)*

##### *Measurement of Oxygen Radicals and Nitric Oxide*

Hearts were perfused with infusion of either the oxygen radical spin trap DMPO (50 mM) or the NO trap  $\text{Fe}^{2+}$ -MGD<sub>2</sub> (Fe-MGD; 1 mM in  $\text{Fe}^{2+}$ , 5 mM in MGD). Effluent was sampled during the minute prior to ischemia (PI) and the first minute of reflow (R). Measurements were performed at 9.77 GHz using a Bruker ER 300 spectrometer in a flat cell and TM<sub>110</sub> cavity with microwave power of 20 mW or 80 mW and modulation amplitude of 0.5 G or 4.0 G, respectively, for the DMPO or Fe-MGD measurements (29).

#### *Western Blot for PARP*

Freshly dissected WT and PARP-1<sup>-/-</sup> heart was homogenized in NP-40 lysis buffer, sonicated for 15 sec, and normalized for protein content with the bicinchoninic acid (BCA) protein assay (Pierce, Rockford, IL). Heart protein (20  $\mu\text{g}$ ) was resolved by SDS-PAGE in each lane of a 4–12% gradient gel and then transferred to nitrocellulose (NC) membrane. To detect PARP protein, NC membrane was probed with rabbit anti-PARP antibody [BioMol (Plymouth Meeting, PA) 1:3500 dilution in 3% bovine serum albumin (BSA)/Tris-Buffered Saline (TBS)] for 2 hr at room temperature with gentle agitation. This was followed by three 5-min washes with 0.5% BSA/TBS and subsequent incubation with goat anti-rabbit HRP-conjugated secondary antibody (Amersham Life Science [Arlington Heights, IL] 1:15,000 dilution in 3% BSA/TBS) for 45 min at room temperature (RT). Labeled protein was visualized through enhanced chemiluminescence with Renaissance Western Blot Chemilu-

minescence Reagent Plus (NEN Life Science Products Boston, MA).

#### *PolyADPribose in situ (PARIS) Detection*

Fresh frozen cryostat sections (10  $\mu\text{m}$ ) from rodent heart, brain and pancreas were allowed to warm to RT and then preincubated at RT in PARIS buffer [56 mM *N*-2-hydroxyethylpiperazine-*N*-2-ethylanesulfonic acid (HEPES) / 28 mM KCl / 28 mM NaCl / 5 mM  $\text{MgCl}_2$  / 0.01% digitonin / 2 mM DTT / 0.5 mM novobiocin, pH 7.5] for 15 min. In control sections, 10  $\mu\text{M}$  3,4-dihydro-5-[4-(1-piperidinyloxy)-1(2H)-isoquinolone (DPQ) or 1 mM benzamide was added to inhibit PARP activity. Liquid was carefully aspirated by gentle vacuum so as not to disturb tissue. Sections were covered with 0.2 ml of PARIS buffer containing 30 nM [ $^{33}\text{P}$ ]  $\text{NAD}^+$  (NEN Life Science Products) and incubated at 4°C for 15 min. After incubation, slides were transferred into staining jars containing 10% trichloroacetic acid at 4°C for 10 min and then dried under cool air. For quantification of PARIS signal, tissue sections were solubilized in 2% SDS / 0.1 M NaOH, normalized for protein content with the bicinchoninic acid protein assay (Pierce), and subjected to scintillation counting of radioactively labeled PAR. Protein content and scintillation counting were obtained in triplicate from at least five different animals and averaged for each sample. To ensure that regional differences in PARP activity were not due to the procedure of sacrificing animals, PARIS was also performed on brain sections dissected from rodent heads that were decapitated directly into liquid nitrogen in order to freeze tissue as rapidly as possible.

#### *In situ End Labeling (ISEL) of Broken DNA*

Fresh frozen cryostat sections (10  $\mu\text{M}$ ) of rodent heart, brain and pancreas were fixed in 4% paraformaldehyde in phosphate-buffered saline (PBS) for 20 min, washed three times for 3 min in 2 $\times$  standard saline phosphate/EDTA [SSPE; 1 $\times$  SSPE = 0.13 NaCl / 10 mM phosphate (pH 7.4) / 1 mM EDTA], and then permeabilized for 20 min in 2 $\times$  SSPE / 0.5% Triton X-100. Slides were washed two times for 3 min in 2 $\times$  SSPE, acetylated 10 min in 0.1 M triethanolamine (pH 8.0), and washed three times for 3 min in 2 $\times$  SSPE. Sections were dehydrated through an ethanol series, dried at RT, and covered with 0.5 ml of reaction mix [0.5 mM dATP, dTTP, dGTP, and [ $^{33}\text{P}$ ] dCTP (NEN Life Science Products)/7.5 units / ml DNA polymerase I (Sigma) in PBS

buffer containing 5 mM  $\text{MgCl}_2$ , 10 mM 2-mercaptoethanol, and 20 mg/ml BSA]. Negative controls that omitted either DNA polymerase I or [ $^{33}\text{P}$ ] dCTP did not show any signal. Slides were incubated at 37°C for 1 hr in a humidified chamber. The reaction was stopped by incubating slides at 65°C in 2 $\times$  SSPE for 2 hr. Slides were then washed three times for 5 min in TBS and dried under cool air. ISEL signal was quantified through scintillation counting of samples normalized for protein content. Results were obtained in triplicate from at least five different animals and averaged for each sample.

#### *Statistical Analysis*

Data are expressed as mean  $\pm$  SEM. Differences in the recovery among groups were determined using a repeated measures two-way analysis of variance with individual comparisons performed by *t*-test.

## Results

### *Myocardial Ischemia-Reperfusion Augments PARP Activity in the Heart*

To investigate the role of polyADPriboseylation in cardiac I/R injury, we subjected WT or PARP-1 $^{-/-}$  isolated perfused mouse hearts to I/R and monitored PARP activity in rat heart slices with the PARIS assay (Fig. 1). With PARIS, [ $^{33}\text{P}$ ]  $\text{NAD}^+$  was converted to PAR and extensive washing with trichloroacetic acid removed the radiolabel that was not covalently incorporated into PAR (8,30). Synthesized PAR was either autoradiographically visualized or quantified through scintillation counting of protein-normalized solubilized tissue sections. All tissues were evaluated in the presence and absence of the PARP inhibitor benzamide (1 mM). PARP activity values were corrected for the small amount of radiolabel detected in the presence of benzamide, which ranged in the heart from 5–12% of values in the absence of benzamide. DPQ, a more potent and selective PARP inhibitor, reduced PARP activity in tissue slices at much lower concentrations (10  $\mu\text{M}$ ) than benzamide (data not shown). I/R increased PARP activity in WT heart by 30% ( $p < 0.001$ ). Inclusion of either SC-55858 (40  $\mu\text{M}$ ; Monsanto St. Louis, MO), a molecular analogue of superoxide dismutase (SOD), or the nitric oxide synthase (NOS) inhibitor, L-NAME, during reperfusion following ischemia reduced PARP activity in injured myocardium

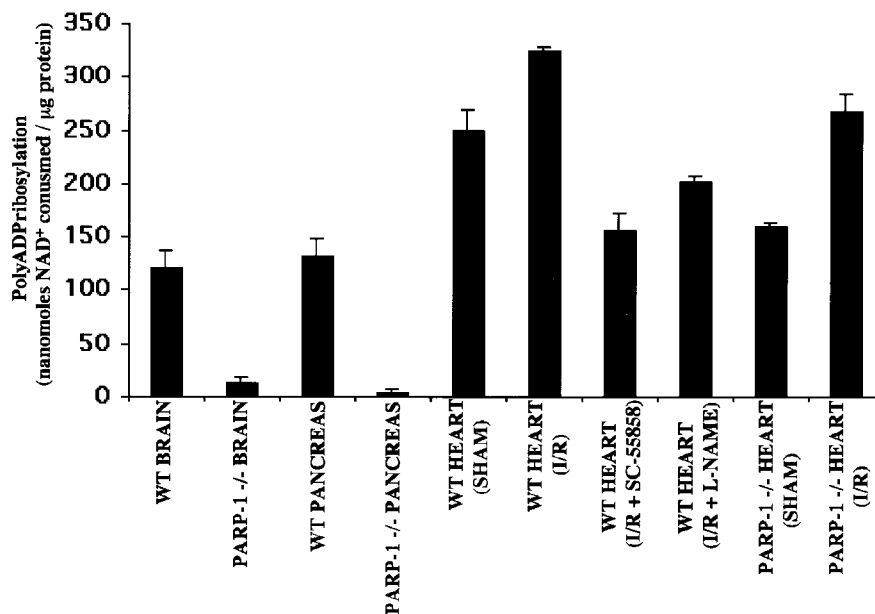


**Fig. 1. Basal polyADPriboseylation in brain, pancreas and heart, and PARP activation in heart after I/R.** WT brain and pancreas show comparable levels of basal PARP activity, with negligible polyADPriboseylation in PARP-1<sup>-/-</sup> brain and pancreas, ( $p < 0.001$ ). Sham-treated WT heart shows roughly twice the amount of basal PARP activity as WT brain and pancreas ( $p < 0.001$ ), and polyADPriboseylation is augmented by 30% following I/R ( $p < 0.01$ ). WT heart PARP activity is decreased to approximately 50% of baseline levels

by 50% and 40%, respectively, relative to WT heart subjected to I/R. These reduced levels of PARP activity were roughly equivalent to basal PARP activity in PARP-1<sup>-/-</sup> hearts, which was reduced only about 30% in sham-treated animals ( $p < 0.01$ ). By contrast, in matched experiments, PARP activity was virtually abolished in PARP-1<sup>-/-</sup> brain and pancreas ( $p < 0.001$ ), ensuring that the PARIS assay in tissue slices validly measured PARP activity. Basal PARP activity in control WT heart was the same as sham-treated WT heart (data not shown). Basal PARP activity in WT brain and pancreas was half that of WT heart, comparable to residual PARP activity in PARP-1<sup>-/-</sup> heart (Fig. 1). Tissue-specific differences in basal PARP activity did not correlate with relative levels of DNA damage, as assessed through <sup>33</sup>P-dCTP ISEL of broken DNA fragments (data not shown). WT brain had twice as much basal DNA damage as WT heart; whereas, WT pancreas had roughly half as much DNA damage as WT heart (unpublished observations by authors AAP, EEC, AV, SHS).

when the superoxide dismutase (SOD) analog SC-55858 (40  $\mu$ M) or the NOS inhibitor L-NAME (1mM) are included in the reperfusion phase ( $p < 0.001$ ). Unlike PARP-1<sup>-/-</sup> brain or pancreas, sham-treated PARP-1<sup>-/-</sup> heart contains approximately 65% of basal polyADPriboseylation seen in sham-treated WT hearts ( $p < 0.01$ ). PolyADPriboseylation in PARP-1<sup>-/-</sup> hearts is augmented by 60% with I/R ( $p < 0.001$ ). WT, wild type; PARP, polyADPribose polymerase; I/R, ischemia-reperfusion.

I/R augmented polyADPriboseylation in PARP-1<sup>-/-</sup> hearts by 60% ( $p < 0.001$ ), which was greater than the percentage increase elicited by I/R in WT heart (Fig. 1). PARP activity in PARP-1<sup>-/-</sup> hearts after I/R was comparable to sham-treated WT hearts.

I/R of WT heart elicited a major increase in PAR immunostaining. PAR staining in sham-treated PARP-1<sup>-/-</sup> hearts was notably less than in WT matched hearts, but still substantial, confirming the residual polyADPriboseylation in PARP-1<sup>-/-</sup> hearts that we observed with the PARIS assay. Also in confirmation of the PARIS data, PAR staining was increased in PARP-1<sup>-/-</sup> hearts after I/R, with levels of staining comparable to sham-treated WT hearts (Fig. 2).

#### *PARP Deletion Preserves Cardiac Contractility, NAD and ATP Stores*

Ischemia elicited a 35% decline in NAD<sup>+</sup> in both WT and PARP-1<sup>-/-</sup> animals. Although reperfusion produced further NAD<sup>+</sup> decline in WT hearts to 40% of control, NAD<sup>+</sup> levels were

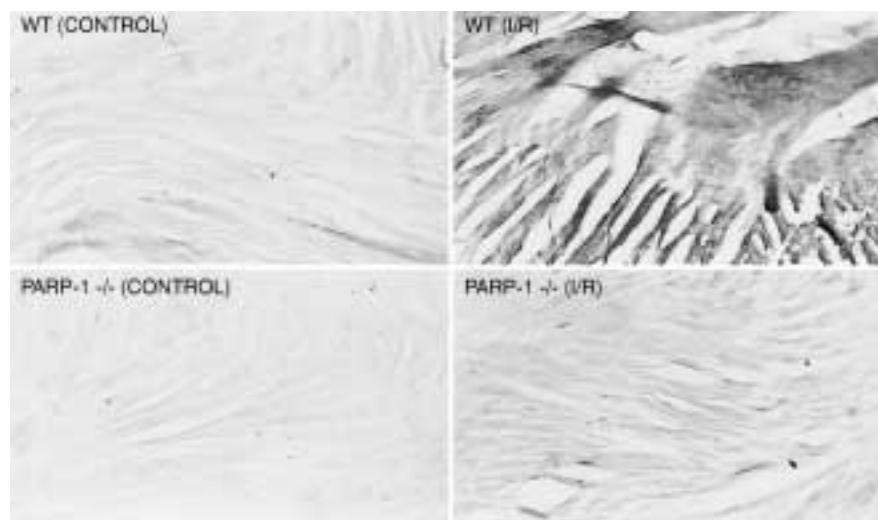


**Fig. 2. Immunohistochemical staining for polyADP-ribose (PAR).** Control hearts were perfused for 40 min with normal saline and experimental hearts underwent 30 min of global ischemia and 10 min of reperfusion. Triplicate hearts were studied for each condition with representative results shown. PAR staining is increased dramatically

following I/R in WT heart. Basal PAR staining in PARP-1<sup>-/-</sup> heart is substantially less than in WT heart. Staining for PAR in PARP-1<sup>-/-</sup> heart increases following I/R to levels that appear comparable to basal PAR staining seen in WT heart. WT = wild type; PARP-1<sup>-/-</sup> = polyADP-ribose polymerase-1 knockout; I/R = ischemia-reperfusion.

stable in PARP-1<sup>-/-</sup> hearts (Fig. 3). ATP levels fell to 20% of control during ischemia in both WT and PARP-1<sup>-/-</sup> hearts. With reperfusion, however, ATP levels remained low in WT hearts, but increased in PARP-1<sup>-/-</sup> hearts to levels about double those of WT (Fig. 3). During reperfusion, phosphocreatine levels in PARP-1<sup>-/-</sup> hearts recovered to values about 20% greater than WT (data not shown), consistent with preservation of NAD<sup>+</sup> and ATP in PARP-1<sup>-/-</sup> tissue.

Following ischemia, cardiac contractility decreased to less than 10% of control values, when measured in terms of the rate-pressure product (RPP; Fig. 3). During reperfusion, contractility in WT hearts increased to about 20% of control values. Substantially higher increases were evident in PARP-1<sup>-/-</sup> hearts, with contractility attaining levels almost 40% of control. Coronary artery flow did not differ between WT and PARP-1<sup>-/-</sup> hearts (Fig. 3), indicating that changes in coronary artery blood flow did not account for changes in NAD<sup>+</sup>, ATP and contractility.

#### *PARP Inhibitors Reduced Myocardial Infarct Size in Rat Heart*

The small size of the mouse heart rendered it difficult to obtain reproducible infarct size following coronary artery ligation, so in mice

infarction was measured following global ischemia, while in rats ischemia was induced by LAD occlusion. We used rats to directly examine the effect of coronary artery occlusion on the dynamics of polyADP-ribose. After occlusion of the LAD for 45 min, followed by 2 hr of reperfusion, immunohistochemical staining revealed a marked augmentation of PAR density (Fig. 4). No increase in PAR signal was seen in non-ischemic left ventricular regions after LAD occlusion (data not shown). We treated rats with the PARP inhibitor 3-aminobenzamide [10 mg/kg intravenously (i.v.)] just prior to reperfusion and observed a reduction in staining of in vivo-accumulated PAR to levels below the basal accumulation of PAR in sham-treated hearts. Similar reductions in staining were observed with the more potent and selective PARP inhibitor GPI6150 when administered at 4 mg/kg i.p. (TW, P Wang, AAP, SHS, JLZ, unpublished report).

We monitored tissue infarction by staining with TTC. 3-aminobenzamide (3-AB) (10 mg/kg i.v.) decreased infarct size by 46%, 4-aminobenzamide (4-AB) (10 mg/kg i.v.) decreased infarct size by 34%, and GPI6150 (4 mg/kg i.p.) decreased infarct size by 52%. Furthermore, infarct size in PARP-1<sup>-/-</sup> hearts was reduced by 35%, compared with WT heart (Fig. 5).

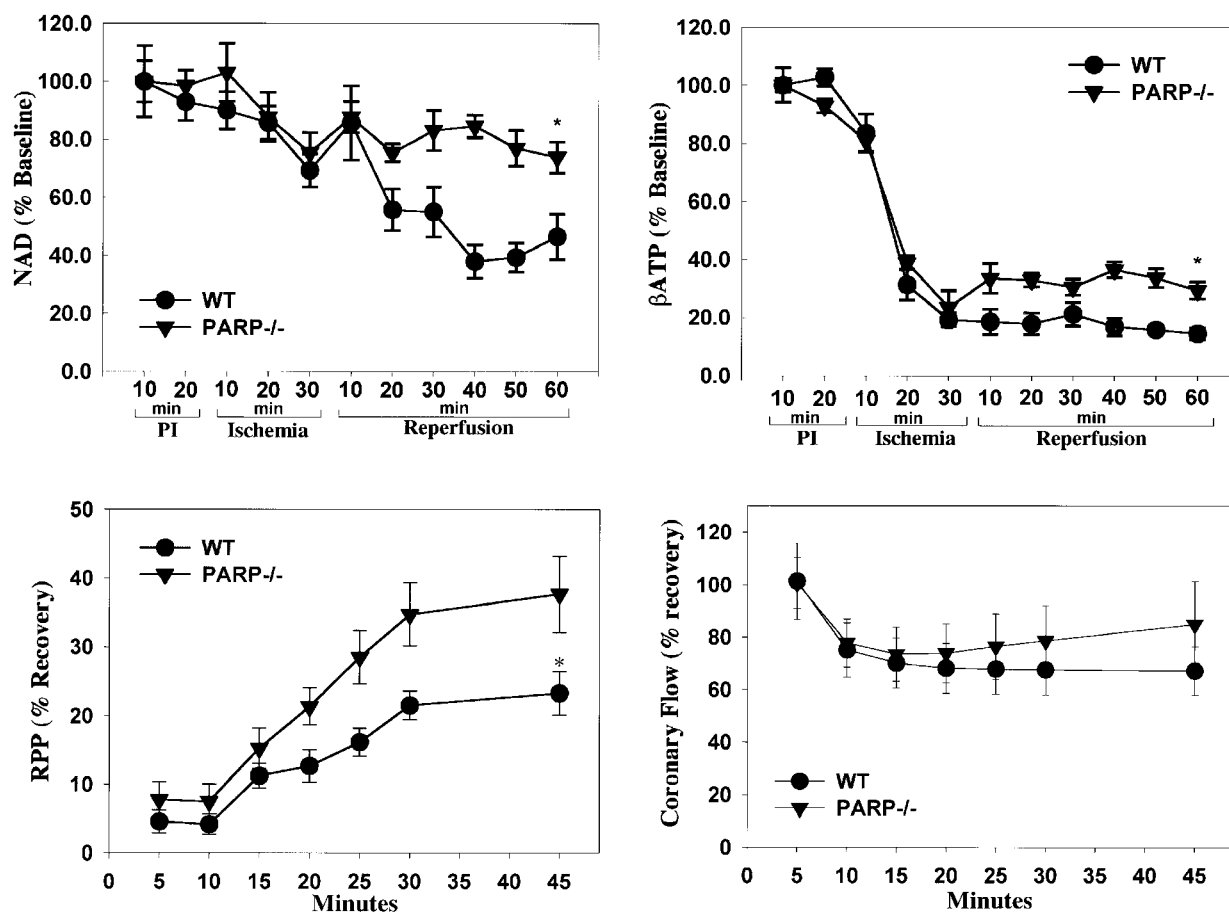


**Fig. 3.** Recovery of energy metabolites and contractile function in WT and PARP-1<sup>-/-</sup> hearts. Hearts were subjected to 30 min of global ischemia, followed by reperfusion. Time courses of changes in NAD<sup>+</sup> and ATP levels are shown in the upper left and right panels, respectively, for WT vs. PARP-1<sup>-/-</sup> ( $p < 0.01$ ). Percent recovery of preischemic values of rate pressure product (RPP), the product of left

ventricular developed pressure and heart rate, which serves as a measure of cardiac work, is shown in the lower left panel. Recovery of coronary flow (CF) is shown in the lower right panel. Values shown are mean  $\pm$  standard error from 7 and 10 hearts, respectively (\*,  $p < 0.05$ ) for WT vs. PARP-1<sup>-/-</sup>. PARP-1<sup>-/-</sup>, polyADPribose polymerase-1 knockout; PI, prior to ischemia; WT, wild type.

#### Ischemia-reperfusion Stimulated Formation of Nitric Oxide and Oxygen Free Radicals

To elucidate factors related to PARP activation, NAD<sup>+</sup> and ATP depletion, and subsequent myocardial cell death after I/R, we monitored formation of NO and reactive oxygen species (ROS). There was abundant evidence that NO and ROS led to DNA damage that activated PARP (7). Both ROS and NO levels increased more than 10-fold from pre-ischemic values during the first 2 min of reflow (Fig. 6).

## Discussion

In this study we have directly demonstrated PARP activation in cardiac tissue following I/R

in isolated-perfused mouse hearts, as well as in rats subjected to coronary artery occlusion. PARP-1<sup>-/-</sup> hearts completely lack PARP-1 enzyme, as determined by Northern blot for PARP-1 mRNA (25) and Western blot for PARP-1 protein (data not shown). We observed substantial residual polyADPriboseylation in PARP-1<sup>-/-</sup> hearts and employed multiple controls to ensure that this validly reflected PARP enzymatic activity. Residual polyADPriboseylation activity presumably reflects a form of PARP other than PARP-1. Recently, new enzymes capable of polyADP-riboseylation have been identified, such as VPARP (31), tankyrase (32), PARP-2 (33), and others (34–39). Although only trace amounts of polyADPriboseylation are detected in PARP-1<sup>-/-</sup> brain or pan-

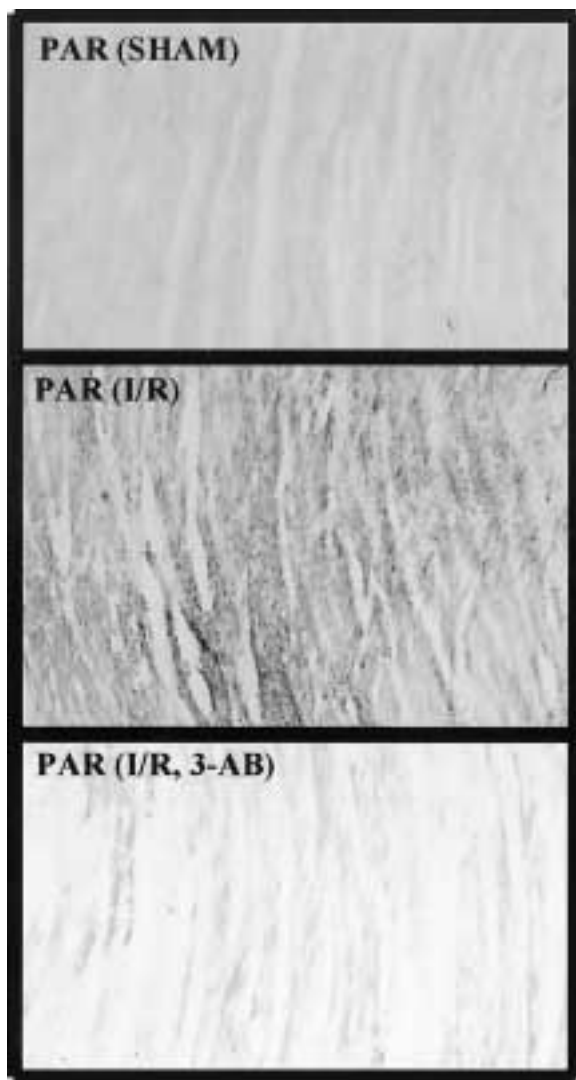


**Fig. 4. Immunohistochemical staining for PAR in rat hearts subjected to in vivo regional I/R with left anterior descending coronary artery (LAD) ligation and 10 min reperfusion.** Myocardium of sham-treated animals exhibits basal levels of PAR staining [PAR (SHAM)] and robust accumulation of PAR in the ischemic risk region of the left ventricle is seen after I/R [PAR (I/R)]. Treatment of rats with the PARP inhibitor, 3-aminobenzamide, prior to reperfusion [PAR (I/R, 3-AB)] reduces in vivo-accumulated PAR to levels below the accumulation of PAR seen in sham-treated hearts. I/R, ischemia-reperfusion; PAR, polyADPribose.

creas, there is significant polyADPribose activity in PARP-1<sup>-/-</sup> heart that is augmented by I/R. We have also observed substantial residual PARP activity in other PARP-1<sup>-/-</sup> tissues, such as testis, lung, skeletal muscle, eye, spleen and kidney (40).

I/R is associated with decreased NAD<sup>+</sup> and ATP, and diminished cardiac contractility. PARP-1 deletion protects against energy loss and subsequent decreased cardiac contractility. In rats, PARP inhibitors prevent myocardial infarct damage. The specific PARP inhibitor, GPI6150, affords greater protection in rats, relative to untreated controls, than PARP-1 deletion does in mouse heart relative to WT. This is consistent with our observations of functional residual polyADPribose in PARP-1<sup>-/-</sup> mouse heart.

Protection against infarct with PARP inhibitors and PARP-1 gene deletion confirms observations of Thiernemann and colleagues (17,18,20,21) that myocardial cell death and loss of contractility following I/R are reduced by PARP inhibition, as well as observations by Szabo and colleagues (19,22,23) of comparable protection in PARP-1<sup>-/-</sup> mouse hearts. Even greater protection against ischemic damage following middle cerebral artery occlusion has been observed in PARP-1<sup>-/-</sup> mice (11,12) and PARP-1<sup>-/-</sup> mice are completely protected from pancreatic damage and subsequent diabetes with streptozotocin (8–10). The substantially greater protection afforded by PARP-1 deletion in pancreas and brain than in heart corresponds with the virtual abolition of polyADPribose in PARP-1<sup>-/-</sup> brain and pancreas, and its partial preservation in PARP-1<sup>-/-</sup> heart. These impressive protective effects suggest that PARP inhibitors may have therapeutic utility in treating vascular stroke, myocardial infarct and Type 1 diabetes.

Our observation of the augmented formation of NO and ROS following I/R fits with other data demonstrating the formation of these substances under similar conditions and supports the notion that ROS and NO are associated with DNA damage (7). NO combines with superoxide to form the more noxious oxidant peroxynitrite, that degenerates to hydroxyl free radical (41). Our experiments delineate a series of events in which ROS presumably damage DNA, leading to PARP activation, which in turn, results in NAD<sup>+</sup> and ATP depletion. The finding that NAD<sup>+</sup> and ATP depletion take place exclusively during reperfusion fits with the notion that this depletion derives from oxidative stimuli. Degradation of ATP during ischemia is thought to lead to the formation of the xanthine oxidase substrates, xanthine and hypoxanthine, which



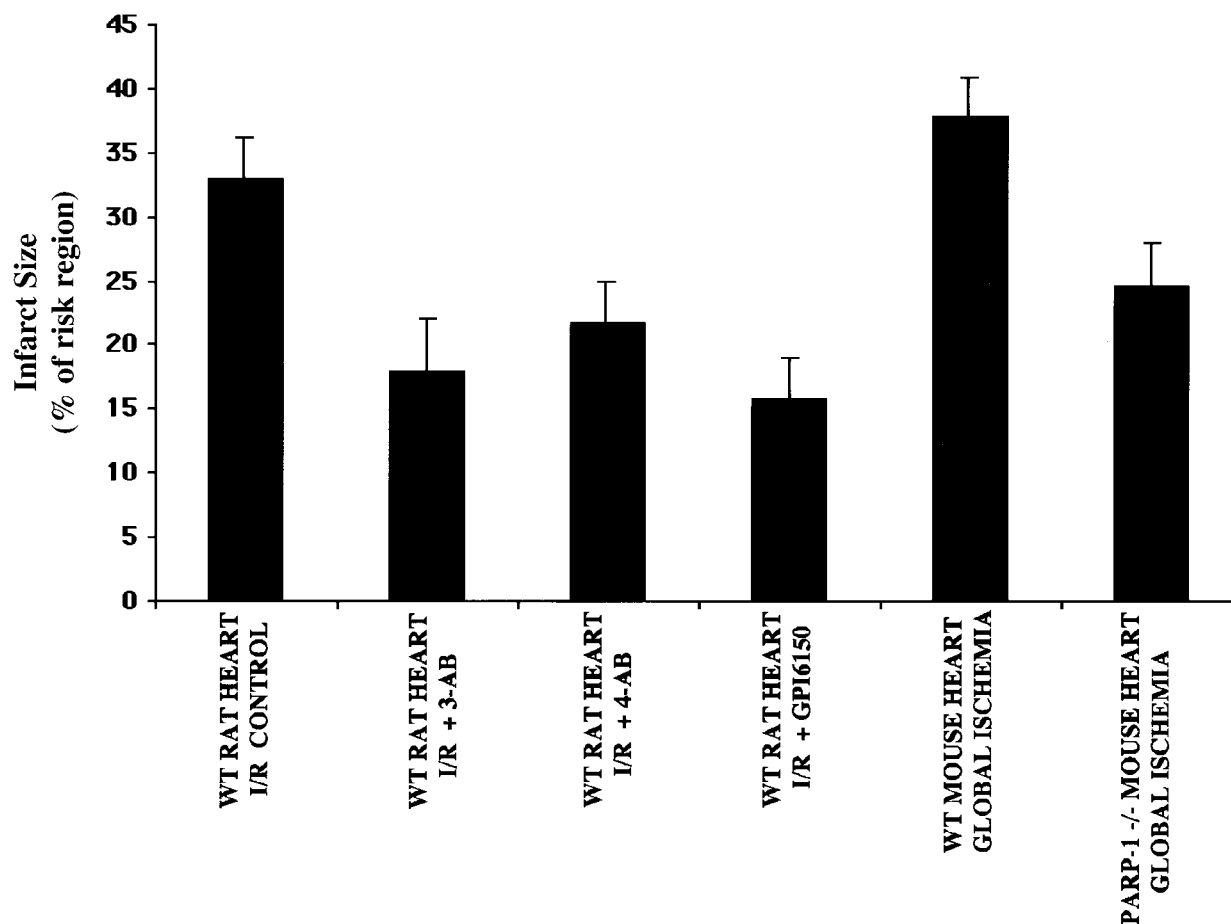


**Fig. 5. Effect of PARP inhibition on in vivo infarct size.** LAD was occluded in female Sprague Dawley (SD) rats for 45 min, followed by 2 hr, reperfusion,  $n = 7$ /group. SD hearts show infarct size of 33% of ischemic LV tissue, which is reduced to 18% with the PARP inhibitor, 3-aminobenzamide, (10 mg/kg i.v.) and 22% with the PARP inhibitor, 4-aminobenzamide, (10 mg/kg i.v.) when administered just prior to reperfusion. Administration of the novel PARP in-

hibitor, GPI 6150, (4 mg/kg i.p., Guilford Pharmaceuticals) 2 hr before ischemia reduces infarct size to 16% of ischemic LV tissue. Infarct size in PARP-1<sup>-/-</sup> mice subjected to global myocardial I/R is decreased by 35% relative to untreated WT mice. WT, wild type; LV, left ventricle; PARP, polyADPribose polymerase; I/R, ischemia-reperfusion; PARP-1<sup>-/-</sup>, PolyADPribose polymerase-1 knockout.

trigger oxygen radical generation from xanthine oxidase (Fig. 6,7). Loss of ATP and decreased phosphorylation potential also lead to intracellular calcium overload, resulting in NO generation, presumably by calcium, with calmodulin directly activating the calcium-calmodulin binding site of NOS. PARP activation following DNA damage leads to consumption of the PARP substrate NAD<sup>+</sup>. NAD<sup>+</sup> is an important coenzyme in energy metabolism and its depletion results in lower ATP production. Furthermore, as the cell tries to compensate by increasing synthesis of NAD<sup>+</sup>, more ATP is consumed. This cycle of ATP depletion com-

promises energy levels of the cell. In a vicious cycle, ATP breakdown also triggers further oxygen radical generation, which may lead to additional DNA damage and PARP activation. Szabo and colleagues (22) observed diminished neutrophil infiltration in PARP-1<sup>-/-</sup> mice, as well as in WT mice treated with the PARP inhibitor 3-aminobenzamide following myocardial I/R. Neutrophil recruitment elicits peroxynitrite formation, so in addition to directly protecting the cell from energy depletion following DNA damage with subsequent PARP activation, PARP inhibition appears to also block up-stream generation of DNA-

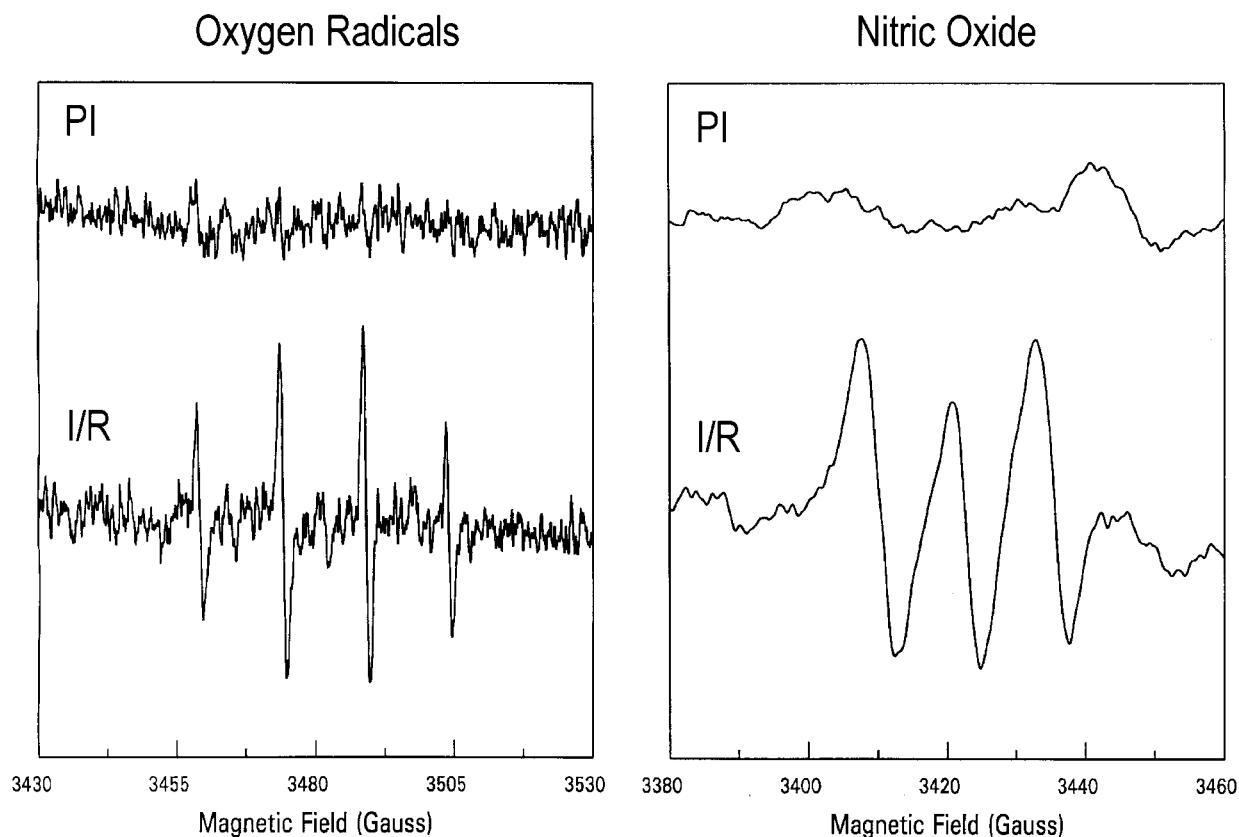


**Fig. 6. Electron paramagnetic resonance (EPR) measurement of oxygen radical and nitric oxide (NO) generation from wild type (WT) hearts.** Hearts were perfused with infusion of either the oxygen radical spin trap 5,5-dimethyl-1-pyrroline-*N*-oxide (DMPO) (50 mM) or the NO trap Fe-*N*-methyl-*D*-glucamine dithiocarbamate (MGD) (1 mM) and effluent sampled both during the minute prior to ischemia (PI) and during the first minute of postischemic reflow (I/R). In triplicate experiments similar results were seen. Prior to ischemia, no detectable oxygen radical signals were detected. After reperfusion, a

prominent 1:2:2:1 quartet of DMPO-OH (hyperfine splitting  $a_N = a_H = 14.9$  G) was present, demonstrating that superoxide/superoxide-derived hydroxyl radicals were formed. Prior to ischemia, only trace NO(Fe-MGD<sub>2</sub>) signals were seen, but after reperfusion, a strong characteristic NO triplet signal ( $g$ -value 2.04,  $a_N = 12.7$  G) was present, indicating increased NO formation. Measurements were performed at 9.77 GHz with microwave power of 20 mW or 80-mW and modulation amplitude of 0.5 G or 4.0 G, respectively, for the DMPO or Fe-MGD measurements.

damaging agents. Thus inhibition of polyAD-Priboseylation may be beneficial in the medical treatment of postischemic myocardial syndromes.

### Acknowledgments

We thank David K. Krug, Dan Guastella, Penghai Wang, and Dr. S. Sankarapandi for technical assistance, and Jan Fertmann for assistance in data preparation. We thank Dr. Jie Zhang, Dr. Ted Dawson, and Dr. Valina Dawson for advice. We thank NEN Life Science

Products for synthesis and donation of [<sup>33</sup>P]NAD<sup>+</sup>. We thank Dr. Z. Q. Wang for generously providing PARP-1<sup>-/-</sup> breeding pairs used to create the colony of mice for this study. This research was supported by NIH grants HL-38324, HL-63744, an American Heart Association Grant in Aid (JLZ), MH-18501, DA-00266, Research Scientist Award DA-00074 (SHS), and NIMH training grant M418 (AAP). One of the authors (SHS) is a consultant, director and member of the scientific advisory board of Guilford Pharmaceuticals, Inc. which is developing drugs based on PARP technology.

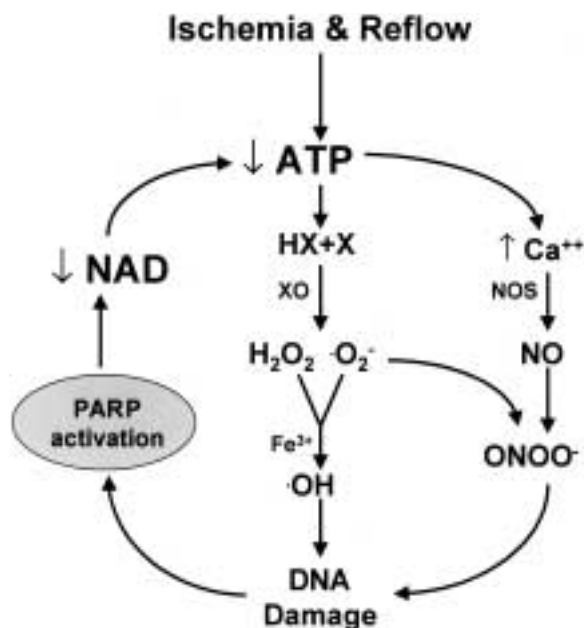


**Fig. 7. Mechanism of PARP activation and its role in cellular energy depletion and injury.** Ischemia causes intracellular ATP depletion that activates pathways of oxygen radical generation, including that from xanthine oxidase. Peroxynitrite and hydroxyl radicals elicit polyADP-ribosylation through damaging DNA. Excessive polyADP-ribosylation depletes intracellular NAD<sup>+</sup>, which can only be replaced at the expense of intracellular ATP pools. This further depletes cellular ATP. As this cycle continues, oxidant injury and ATP depletion result in accumulated cellular injury and death. NO, nitric oxide; NOS, nitric oxide synthase; PARP, polyADP-ribose polymerase.

## References

- de Murcia JM, Niedergang C, Trucco C, et al. (1997) Requirement of poly (ADP-ribose) polymerase in recovery from DNA damage in mice and in cells. *Proc. Natl. Acad. Sci. U.S.A.* **94**: 7303–7307.
- Masson M, Niedergang C, Schreiber V, Muller S, Menissier-de Murcia J, de Murcia, G. (1998) XRCCI is specifically associated with poly (ADP-ribose) polymerase and negatively regulates its activity following DNA damage. *Mol. Cell Biol.* **18**: 3563–3571.
- Leist M, Single B, Kunstle G, Volbracht C, Hentze H, Nicotera P. (1997) Apoptosis in the absence of poly-(ADP-ribose) polymerase. *Biochem. Biophys. Res. Commun.* **233**: 518–522.
- Wang ZQ, Stingl L, Morrison C, et al. (1997) PARP is important for genomic stability but dispensable in apoptosis. *Genes Dev.* **11**: 2347–2358.
- Oliver FJ, de la Rubia G, Rolli V, Ruiz-Ruiz MC, de Murcia G, Murcia JM. (1998) Importance of poly (ADP-ribose) polymerase and its cleavage in apoptosis. Lesson from an uncleavable mutant. *J. Biol. Chem.* **273**: 33533–33539.
- Berger, NA. (1985) Poly (ADP-ribose) in the cellular response to DNA damage. *Radiat. Res.* **101**: 4–15.
- Pieper AA, Verma A, Zhang J, Snyder, SH. (1999) Poly (ADP-ribose) polymerase, nitric oxide, and cell death. *Trends Pharmacol. Sci.* **20**: 171–181.
- Pieper AA, Brat DJ, Krug DK, et al. (1999) Poly (ADP-ribose) polymerase-deficient mice are protected from streptozotocin-induced diabetes. *Proc. Natl. Acad. Sci. U.S.A.* **96**: 3059–3064.
- Burkart V, Wang ZQ, Radons J, et al. (1999) Mice lacking the poly(ADP-ribose) polymerase gene are resistant to pancreatic beta-cell destruction and diabetes development induced by streptozotocin. *Nat. Med.* **5**: 314–319.
- Masutani M, Suzuki H, Kamada N, et al. (1999) Poly (ADP-ribose) polymerase gene disruption conferred mice resistant to streptozotocin-induced diabetes. *Proc. Natl. Acad. Sci. U.S.A.* **96**: 2301–2304.
- Eliasson MJL, Sampei K, Mandir AS, et al. (1997) Poly (ADP-ribose) polymerase gene disruption renders mice resistant to cerebral ischemia. *Nat. Med.* **3**: 1089–1095.
- Endres M, Wang ZQ, Namura S, Waeber C, Moskowitz MA (1997) Ischemic brain injury is mediated by the activation of poly (ADP-ribose) polymerase. *J. Cereb. Blood Flow Metab.* **17**: 1143–1151.
- Takahashi K, Greenberg JH, Jackson P, Maclin K, Zhang J. (1997) Neuroprotective effects of inhibiting poly (ADP-ribose) synthetase on focal cerebral ischemia in rats. *J. Cereb. Blood Flow Metab.* **17**: 1137–1142.
- Tokime T, Nozaki K, Sugino T, Kikuchi H, Hashimoto N, Ueda, K. (1998) Enhanced poly (ADP-ribosylation) after focal ischemia in rat brain. *J. Cereb. Blood Flow Metab.* **18**: 991–997.
- Gilad E, Zingarell, B, Salzman AL, Szabo C. (1997) Protection by inhibition of poly (ADP-ribose) synthetase against oxidant injury in cardiac myoblasts In vitro. *Mol. Cell Cardiol.* **29**: 2585–2597.
- Bowes J, Piper J, Thiernemann C. (1998) Inhibitors of the activity of poly (ADP-ribose) synthetase reduce the cell death caused by hydrogen peroxide in human cardiac myoblasts. *Br. J. Pharmacol.* **124**: 1760–1766.
- Bowes J, McDonald MC, Piper J, Thiernemann C. (1999) Inhibitors of poly (ADP-ribose) synthetase protect rat cardiomyocytes against oxidant stress. *Cardiovasc. Res.* **41**: 126–134.
- Bowes J, Ruetten H, Martorana PA, Stockhausen H, Thiernemann C. (1998) Reduction of myocardial reperfusion injury by an inhibitor of poly (ADP-ribose) synthetase in the pig. *Eur. J. Pharmacol.* **359**: 143–150.

19. Zingarelli B, Cuzzocrea S, Zsengeller Z, Salzman AL, Szabo C. (1997) Protection against myocardial ischemia and reperfusion injury by 3-aminobenzamide, an inhibitor of poly (ADP-ribose) synthetase. *Cardiovasc. Res.* **36**: 205–215.
20. Thiernemann C, Bowes J, Myint FP, Vane JR. (1997) Inhibition of the activity of poly (ADP-ribose) synthetase reduces ischemia-reperfusion injury in the heart and skeletal muscle. *Proc. Natl. Acad. Sci. U.S.A.* **94**: 679–683.
21. Docherty JC, Kuzio B, Silvester JA, Bowes J, Thiernemann C. (1999) An inhibitor of poly (ADP-ribose) synthetase activity reduces contractile dysfunction and preserves high energy phosphate levels during reperfusion of the ischaemic rat heart. *Br. J. Pharm.* **127**: 1518–1524.
22. Zingarelli B, Salzman AL, Szabo C. (1998) Genetic disruption of poly (ADP-ribose) synthetase inhibits the expression of P-selectin and intercellular adhesion molecule-1 in myocardial ischemia/reperfusion injury. *Circ. Res.* **83**: 85–94.
23. Grupp IL, Jackson TM, Hake P, Grupp G, Szabo C. (1999) Protection against hypoxia-reoxygenation in the absence of poly (ADP-ribose) synthetase in isolated working hearts. *J. Mol. Cell Cardiol.* **31**: 297–303.
24. Shinobu LA, Jones SG, Jones MM. (1984) Sodium N-methyl-D-glucamine dithiocarbamate and cadmium intoxication. *Acta. Pharmacol. Toxicol. (Copenh.)* **54**: 189–194.
25. Wang ZQ, Auer B, Stingl L, et al. (1995) Mice lacking ADPRT and poly (ADP-ribosylation) develop normally but are susceptible to skin disease. *Genes Dev.* **9**: 509–520.
26. Wang P, Chen H, Qin H, et al. (1998) Overexpression of human copper, zinc-superoxide dismutase (SOD1) prevents postischemic injury. *Proc. Natl. Acad. Sci. U.S.A.* **95**: 4556–4560.
27. Curtis MJ, Macleod BA, Walker MJ. (1987) Models for the study of arrhythmias in myocardial ischaemia and infarction: the use of the rat. *J. Mol. Cell Cardiol.* **19**: 399–419.
28. Fishbein MC, Meerbaum S, Rit J, et al. (1981) Early phase acute myocardial infarct size quantification: validation of the triphenyl tetrazolium chloride tissue enzyme staining technique. *Am. Heart J.* **101**: 593–600.
29. Xia Y, Zweier JL. (1995) Substrate control of free radical generation from xanthine oxidase in the postischemic heart. *J. Biol. Chem.* **270**: 18797–18803.
30. LaPlaca MC, Raghupathi R, Verma A, et al. (1999) Temporal patterns of poly (ADP-ribose) polymerase activation in the cortex following experimental brain injury in the rat. *J. Neurochem.* **73**: 205–213.
31. Kickhoefer VA, Siva AC, Kedersha NL, et al. (1999) The 193-kD vault protein, VPARP, is a novel poly (ADP-ribose) polymerase. *J. Cell Biol.* **146**: 917–928.
32. Smith S, Giriat I, Schmitt A, deLange T. (1998) Tankyrase, a poly (ADP-ribose) polymerase at human telomeres. *Science* **282**: 1484–1487.
33. Ame JC, Rolli V, Schreiber V, et al. (1999) PARP-2, a novel mammalian DNA damage-dependent poly (ADP-ribose) polymerase. *J. Biol. Chem.* **274**: 17860–17868.
34. Shieh WM, Ame JC, Wilson MV, et al. (1998) Poly (ADP-ribose) polymerase null mouse cells synthesize ADP-ribose polymers. *J. Biol. Chem.* **273**: 30069–30072.
35. Johansson M. (1999) A human poly (ADP-ribose) polymerase gene family (ADPRTL): cDNA cloning of two novel poly (ADP-ribose) polymerase homologues. *Genomics* **57**: 442–445.
36. Kawamura T, Hanai S, Yokota T, et al. (1998) An alternative form of poly (ADP-ribose) polymerase in *Drosophila melanogaster* and its ectopic expression in rat-1 cells. *Biochem. Biophys. Res. Commun.* **251**: 35–40.
37. Lepiniec L, Babychuk E, Kushnir S, Van Mantagu M, Inze D. (1995) Characterization of an Arabidopsis thaliana cDNA homologue to animal poly (ADP-ribose) polymerase. *FEBS Lett.* **364**: 103–108.
38. Babychuk E, Cottrill PB, Storozhenko S, et al. (1998) Higher plants possess two structurally different poly (ADP-ribose) polymerases. *Plant J.* **15**: 635–645.
39. Berghammer H, Ebner M, Marksteiner R, Auer B. (1999) pADPRT-2: a novel mammalian polymerizing (ADP-ribosyl)transferase gene related to truncated pADPRT homologues in plants and *Caenorhabditis elegans*. *FEBS Lett.* **449**: 259–263
40. Pieper AA, Blackshaw S, Clements EE, et al. (2000) Basal in vivo DNA damage activating poly (ADP-ribosylation) reflects glutamate-nitric oxide neurotransmission. *Proc. Natl. Acad. Sci. U.S.A.* **97**: 1845–1850.
41. Szabo C. (1996) DNA strand breakage and activation of poly-ADP ribosyltransferase: a cytotoxic pathway triggered by peroxynitrite. *Free Radic. Biol. Med.* **21**: 855–869.